ELSEVIER

Ceramics International 33 (2007) 1075–1081

CERAMICS INTERNATIONAL

www.elsevier.com/locate/ceramint

Heat treatment of nanostructured thermal barrier coating

Na Wang, Chungen Zhou *, Shengkai Gong, Huibin Xu

Department of Materials Science and Engineering, Beijing University of Aeronautics Astronautics, Beijing 100083, China

Received 25 September 2005; received in revised form 13 February 2006; accepted 20 March 2006

Abstract

A nanostructured thermal barrier coating has been prepared by air plasma spraying using YSZ (8 wt% Y_2O_3 partially stabilized zirconia) nano powder. The effect of annealing on the nanostructured zirconia coating has been investigated. The grain size of the nanostructured zirconia coating increased with increasing annealing time and temperature. Grains grew with preferential direction and into a columnar structure. The growth activation energy in the nanocrystalline grains is very low, which comes from existence of micro-pores in the coating and the grain-rotation-induced grain coalescence (GRIGC) mechanism.

Keywords: Nanostructure; Annealing; Thermal barrier coating; Plasma spraying

1. Introduction

Thermal barrier coatings (TBCs) have been widely used since the 1970s to insulate metallic components in gas-turbine and diesel engines from high temperatures. These coatings can prolong the lifetime of the component and increase allowable operating temperatures [1]. A typical duplex TBC system consists of a thermally insulating ceramic top coat and an oxidation-resistant metallic bond coat applied over a metal substrate providing structural strength. A thermally grown oxide (TGO) would form between the ceramic top coat and the bond coat due to high temperature oxidation of the bond coat. The YSZ coatings are commonly used as top coating because of their low thermal conductivity and high coefficient of thermal expansion. MCrAlY (M=Ni, and/or Co) is used as a bond coat to provide a good thermal expansion match between the top coat and substrate and inhibit oxidation of the substrate. It is reported that the development of high efficient engine requires TBCs of lower thermal conductivity to ensure a high degree of thermal insulation and good strain tolerance to relieve the residual thermal stresses generated during engine operation.

In recent years, the nanostructured zirconia ceramic coatings have been focused on. The nanostructured YSZ may enhance the performance of the TBCs due to its low thermal conductivity, high coefficient of thermal expansion and excellent mechanical properties of this kind of coating [2–7]. However, few reports on plasma-sprayed nanostructured zirconia coatings have been published. In this paper, an interest has been focused on the influence of heat treatment on the grain growth of the YSZ coating for providing the relevant knowledge.

2. Experimental procedures

An 8 wt% Y_2O_3 partially stabilized nanostructured zirconia powder, having grain size of 15–35 nm, was sprayed (APS) on the stainless steel. The size distribution of the agglomerated nano-sized particles is 40–60 μm. Then, the sample used for annealing was put into cooled water immediately after the air plasma spraying has been done. The coating has been detached from the stainless steel, and was 1 mm in thickness. The temperature of the substrate and coating during the plasma spraying was about 300–400 °C because of air cooling. The plasma spraying parameters are given in Table 1.

The heat-treatment tests were performed for 15 h at 600, 800, 900, 1000, 1100, 1150, and at 1100 °C for 15, 25, 45, 70, 100, and 300 h, respectively.

Crystalline species in zirconia powders and coatings after heat treatment were characterized using a D/max 2200pc X-ray diffractometer (Cu Kα radiation; Rigaku, Tokyo, Japan).

---

* Corresponding author. Tel.: +86 108 231 6000; fax: +86 10 82338200.
E-mail address: cgzhou@buaa.edu.cn (C. Zhou).

0272-8842/$32.00 © 2006 Elsevier Ltd and Techna Group S.r.l. All rights reserved.
doi:10.1016/j.ceramint.2006.03.022

Table 1
Plasma-spray parameters for nanostructured zirconia coating

Power (kW)	28
Current (*A*)	560
Voltage (*V*)	50
Primary gas (Ar) (slpm)[a]	60
Secondary gas (H_2) (slpm)[a]	1
Carrier gas (Ar) (slpm)[a]	5
Spraying distance (mm)	80
Feed rate (g min^{-1})	25
Injector internal diameter (mm)	1.5
Injector position to the torch axis (mm)	6
Injector position to the nozzle exit (mm)	8.5

[a] splm: Standard liter per minute.

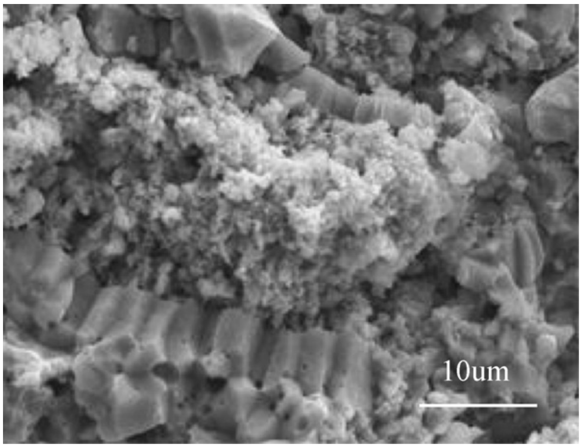

Fig. 1. SEM microstructure of the as-sprayed zirconia coating.

The mean grain sizes of coatings were calculated using the Scherrer equation [8,9]:

$$B_p(2\theta) = \frac{0.9\lambda}{D\cos\theta}$$

where D is the average dimension of crystallite, B_p (2θ) the broadening of the diffraction line measured at the half maximum intensity, λ (0.154 nm) and θ denotes the wavelength of the X-rays and the Bragg diffraction angle, respectively.

The microstructures of the nanostructured zirconia coatings were determined with a S-3500 scanning electron microscope (Hitachi, Tokyo, Japan) and a H-800 transmission electron microscope (Hitachi).

3. Results and discussion

3.1. Microstructure of as-sprayed nanostructured thermal barrier coating

Fig. 1 presents the microstructure of as-sprayed nanostructured zirconia coating revealed in fractured cross-section. It can be seen from Fig. 1 that there are two kinds of structures in the coating: the continuous molten phase and the loose microstructure. It can be seen that the structure is very loose, and the micro-pores between the micro-particles have sizes similar to those of nano-particles. This structure will enhance the thermal insulation property of TBCs [4,7]. The TEM image reveals the grain size of primitive particles and the as-sprayed coating, as shown in Fig. 2. It is seen that the non-molten phase of the coatings are composed of fine grains with sizes ranging from 30 to 50 nm. No smaller grains were found in TEM image.

3.2. Effect of annealing temperature and time on grain size

Fig. 3 gives the XRD patterns of as-deposited coatings before and after annealing treatment at different temperatures for 15 h and at 1100 °C for different times. The coatings before and after annealing consist of tetragonal phase zirconia, indicating that the phase transformation within the coating did not occur during the annealing.

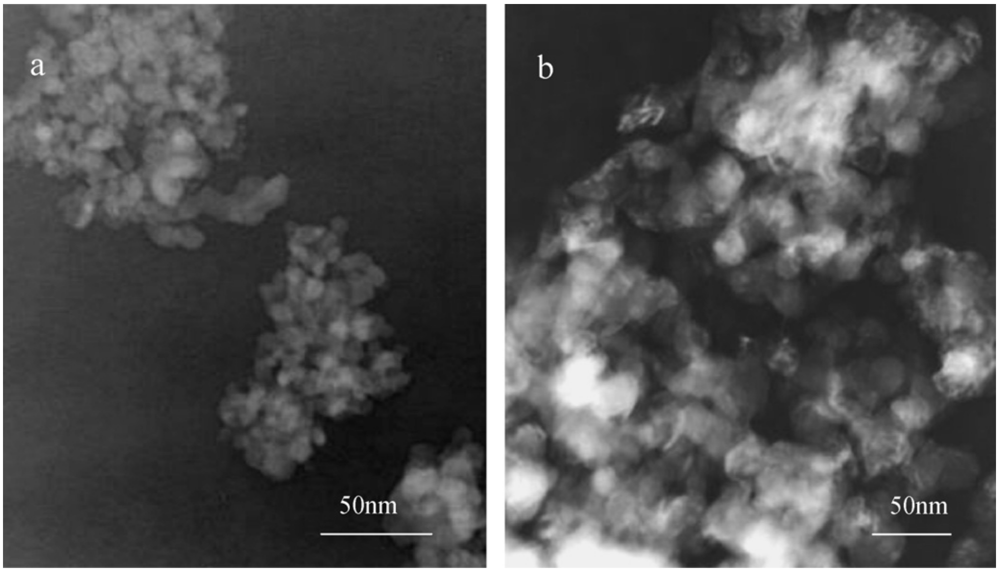

Fig. 2. TEM image of the primitive nano YSZ particles (a) and the as-sprayed coating (b).

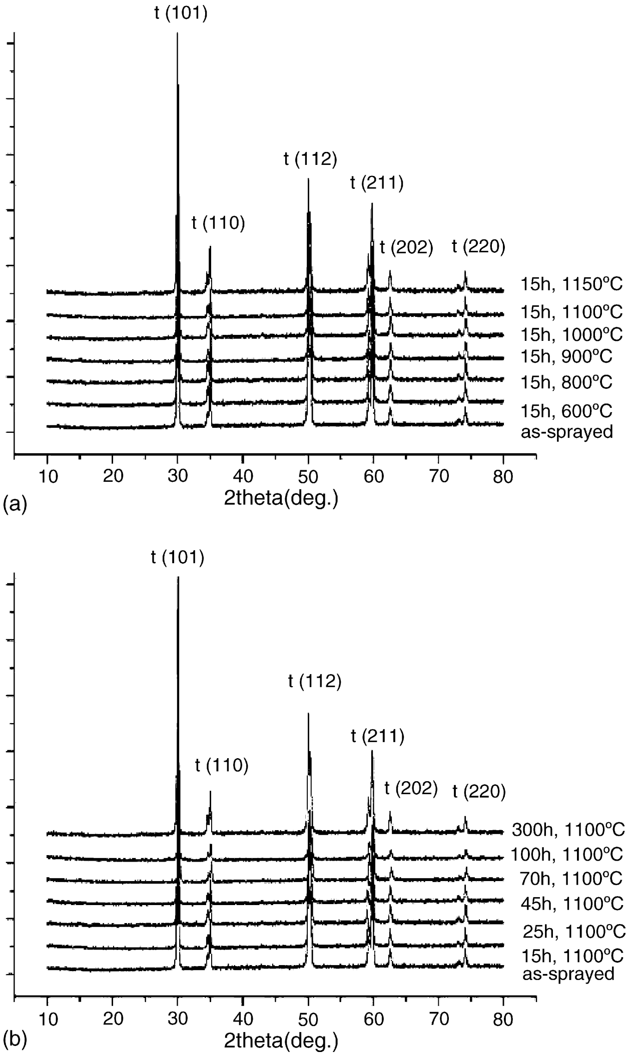

Fig. 3. XRD patterns of the as-sprayed coating and the coatings after heat treatment (a) samples after heat treatment for 15 h at different temperatures (b) samples after heat treatment at 1100 °C for different times.

The mean grain sizes of zirconia coatings were calculated using the Scherrer equation from the results of XRD after heat treatment at different temperatures for 15 h and at 1100 °C for different times, as shown in Fig. 4. It is seen that the calculated grain size of the as-deposited coating is about 57 nm, which coincided with the transmission microscopy observation. The grain sizes of the nanostructured zirconia coating increase with increasing annealing temperature, the average grain size changes from 57 to 88 nm. The annealing time increases, merely the same regularity for the grain growth from 57 to 177 nm.

The activation energy of grain growth within nanostructured TBC was deduced from Fig. 4(a). It was assumed that the grain growth in the nanostructured zirconia coating was thermally activated according to the following equation:

$$D_t = D_0\exp\left(\frac{-Q}{RT}\right)$$

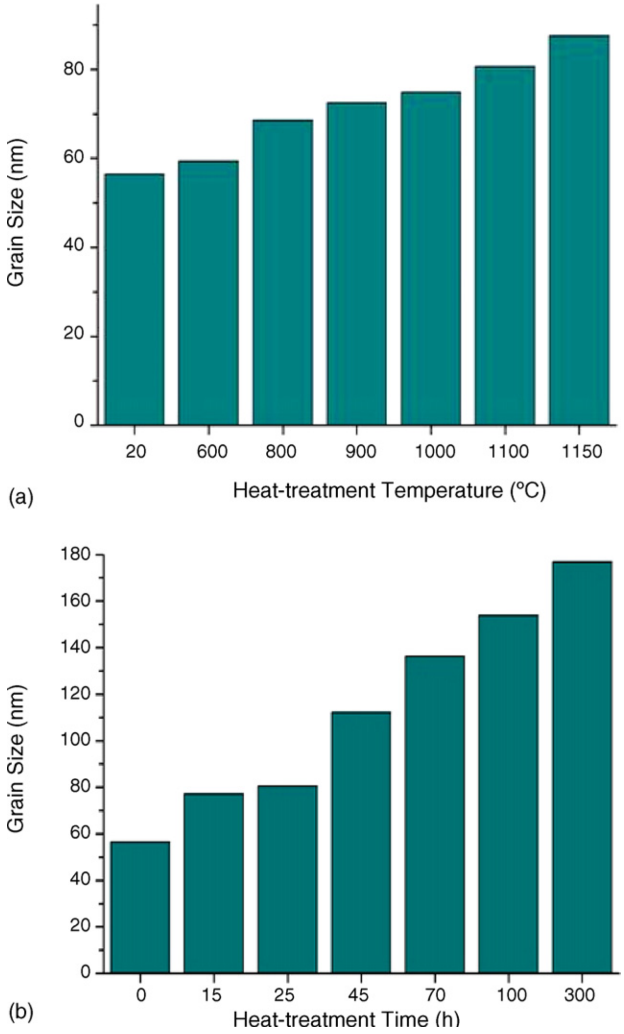

Fig. 4. Grain sizes of YSZ coatings after heat treatment for 15 h at different temperatures (a) and at 1100 °C for different times (b).

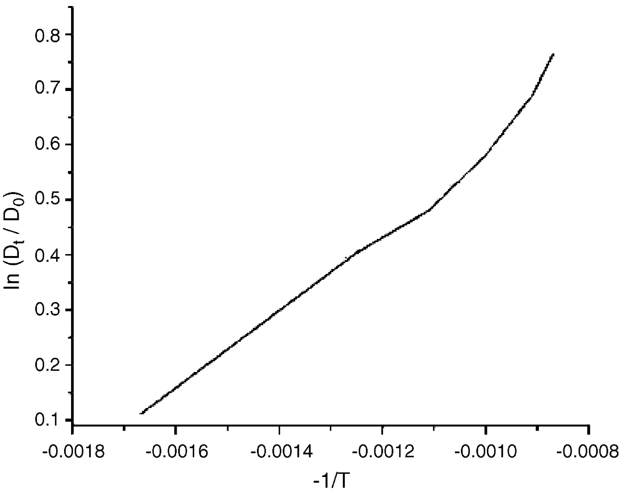

Fig. 5. Variation of ln (D_t/D_0) with minus reciprocal of the temperature.

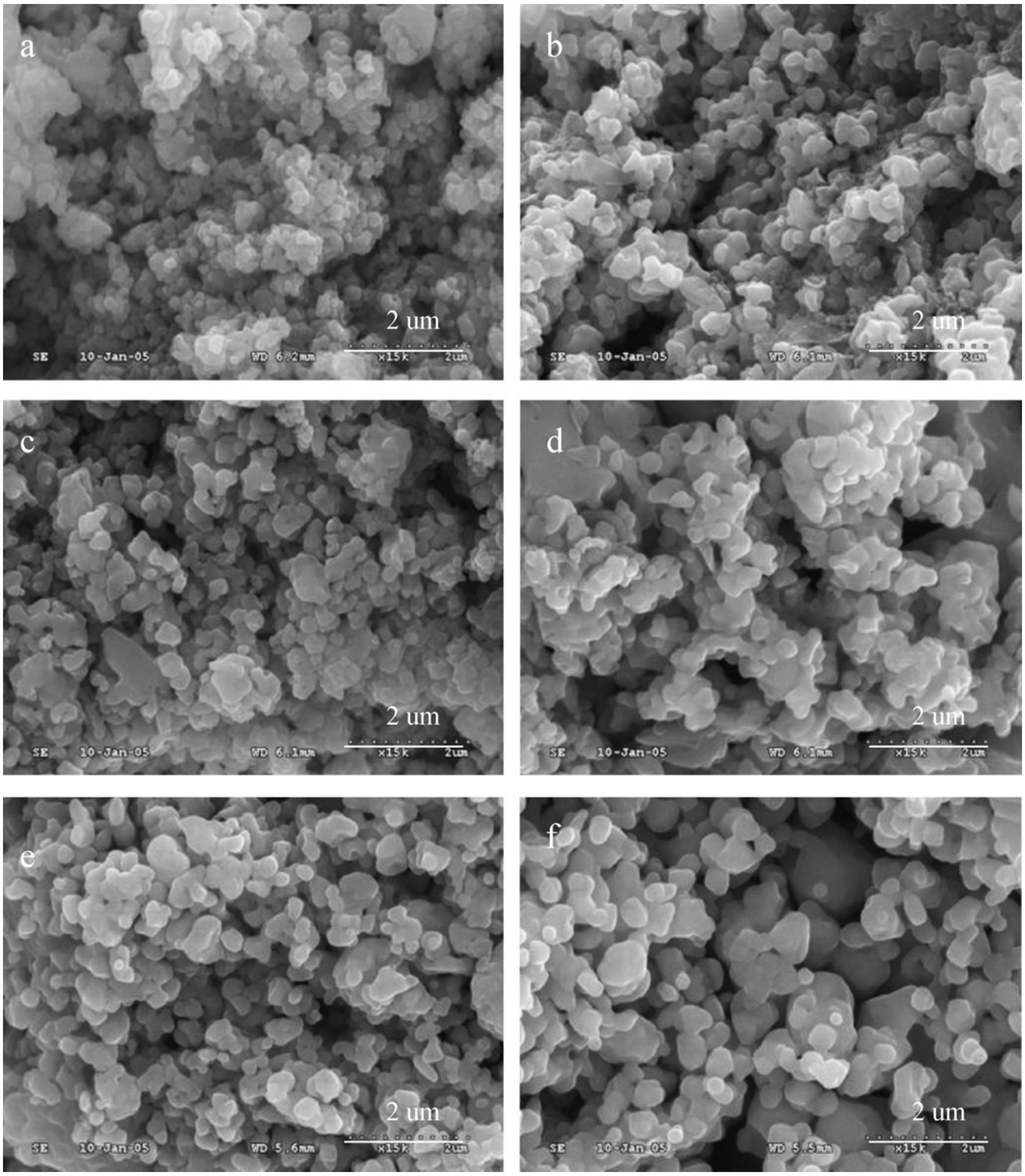

Fig. 6. Surface morphology of the nano YSZ coatings at different temperature after heat treatment for 15 h (a) as-sprayed state, (b) 600 °C, (c) 800 °C, (d) 900 °C, (e) 1000 °C, and (f) 1150 °C.

where D_0 and D_t denote the initial and final nanocrystallite sizes, R is the mol gas constant and T is the annealing temperature. Fig. 5 shows the variation of $\ln(D_t/D_0)$ with minus reciprocal of the temperature. Hence, the activation energy of grain growth can be obtained from the graph of Fig. 5 and is calculated to be 6.5 kJ/mol, which is much lower than that observed for bulk YSZ (580 kJ/mol) [10]. Similar observation has also been reported for other ceramics, namely, ZnO, where the growth activation energy in the nanocrystalline grains is observed to be ~20 kJ/mol, while that for microcrystalline grains is observed to be ~275 kJ/mol. It is obvious that the very low activation energy of grain growth appears to be a characteristic feature of nanocrystalline ceramic oxides [11].

3.3. *Effect of annealing on the morphology*

Details of the microstructural features before and after annealing were examined through SEM observation on the surface of top coat. Fig. 6 presents the surface morphology of nanostructured zirconia coatings in the as-sprayed state and after heat-treating at different temperatures for 15 h. The as-sprayed microstructure is composed of the nano-powders and micro-pores between the nano-powders. The size of the nano-powders increases after annealing at different temperatures for 15 h.

Further details of the microstructural features of the nanostructured zirconia coating after annealing were examined through fractured surfaces of coating. The microstructure of the

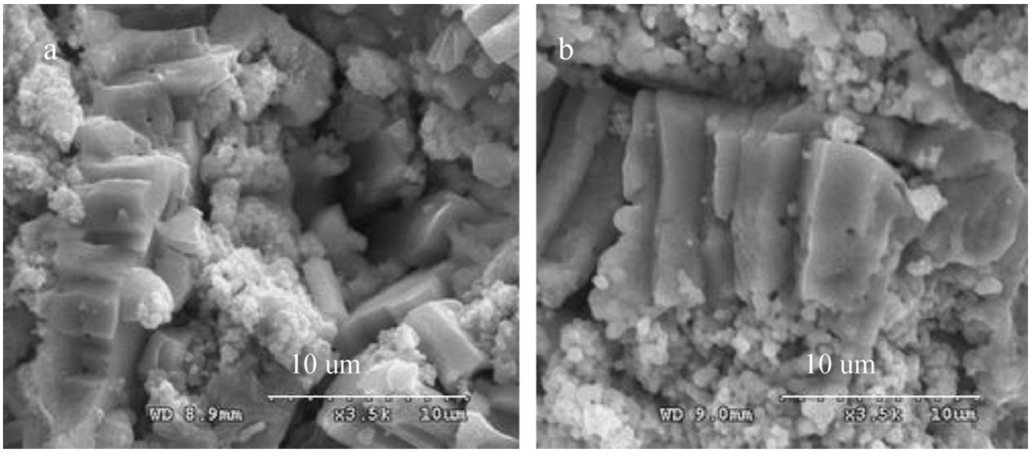

Fig. 7. Microstructure of nanostructured zirconia coating revealed in this fracture cross-section after annealing at 900 °C (a) and 1100 °C (b) for 15 h.

coating after annealing was composed of lamellae and nano-particles (Fig. 7). After annealing, each lamella has a length of about 3–15 μm and thickness of about 0.5–2 μm, as shown in Figs. 7 and 8. As mentioned, the mean grain size had been calculated from the results of XRD. The size of the nano-particles increases, the length and thickness of each lamella may also increase, which resulted from the change of the mean grain size from 57 to 88 nm with increasing temperature and 57 to 188 nm with increasing time. Different locations of the fractured coating exhibit similar results.

Fig. 9 presents the surface morphology of nanostructured zirconia coatings in the as-sprayed state and after heat-treating at 1100 °C for different times. The as-sprayed microstructure was composed of the nano-particles and micro-pores between them. The size of the nano-particles increases with increasing annealing time.

The fractured surfaces of the coating were examined, as shown in Fig. 8. They also are composed of lamellae and nano-particles. Further, these lamellae consist of columnar grains, grown from bottom to the top of the lamellae, indicating that grains grew with preferential direction and into columnar structure after heat-treating for 100 and 300 h at 1100 °C, and the original nanostructure would disappear after a long heat treatment at high temperature. Therefore, in order to obtain high temperature stability, the starting powders must be doped with some phase stabilizer.

The very low activation energy value of ∼6.5 kJ/mol observed in this study mainly comes from two aspects' contribution for the grain growth behavior. First, the existence of micro-pores in the coating makes the surface energy increase drastically and decreases the growth activation energy of nano-particles. After this step, the grain-rotation-induced grain coalescence (GRIGC) mechanism [12,13] must be considered during the growth of nanocrystalline colloidal oxide. According to this model, the rotation of grains among neighboring grains results in a coherent grain–grain interface, which leads to the coalescence of neighboring grains via the elimination of common grain boundaries. A rotation process, which presents very low activation energy or even a zero-kinetic barrier according to the GRIGC mechanism, may occur to decrease the angle of misorientation and change the grain's orientation. In the present investigation, the grain morphology showed preferential growth during the annealing. This result indicates that the GRIGC mechanism occurs.

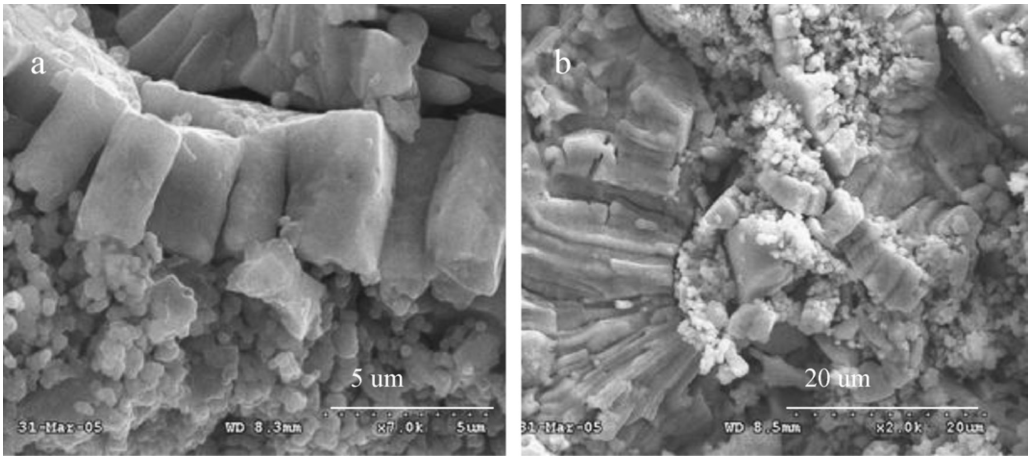

Fig. 8. Microstructure of nanostructured zirconia coating revealed in this fracture cross-section after annealing at 1100 °C for 100 h (a) and 300 h (b).

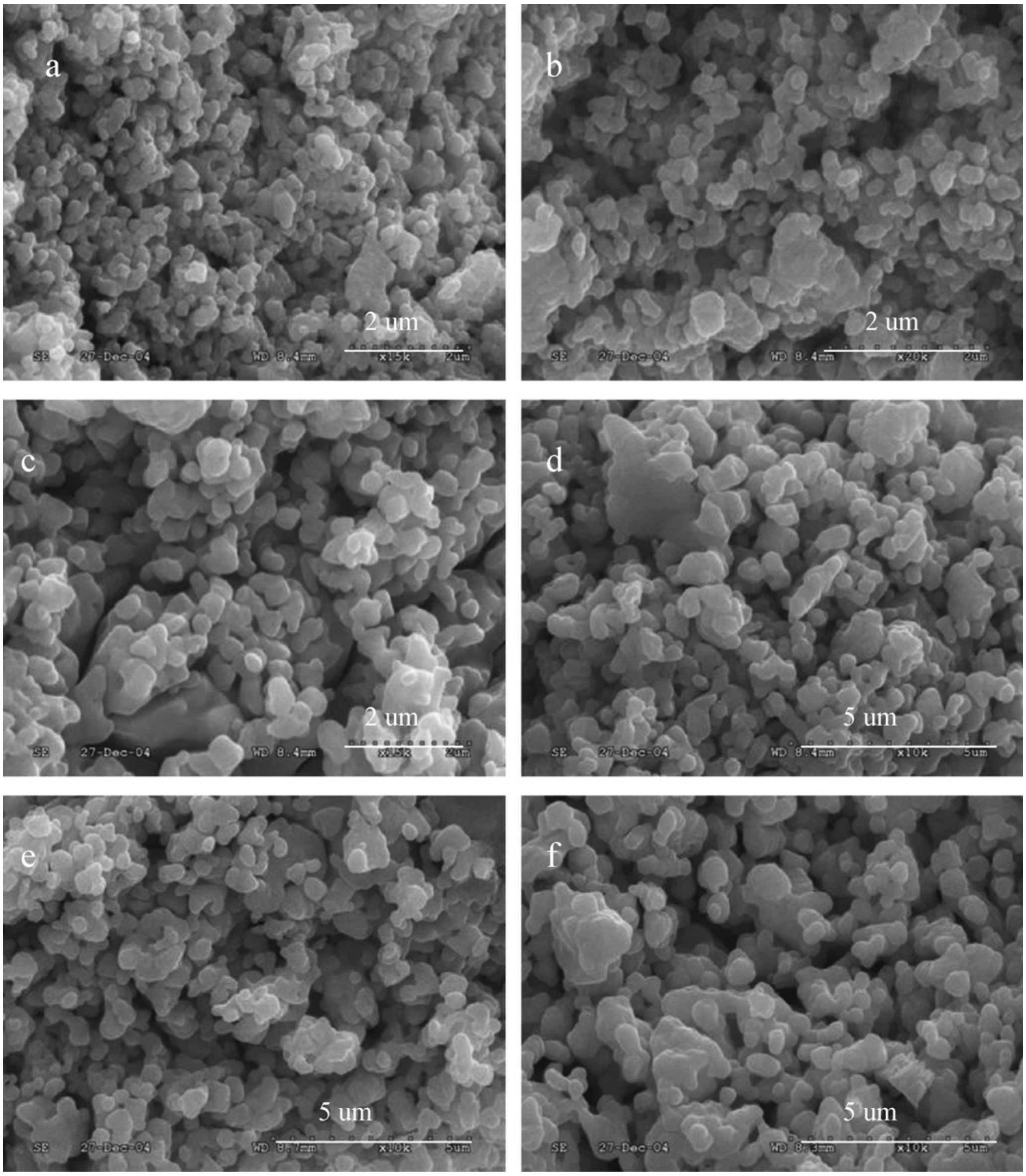

Fig. 9. Surface morphology of the nano YSZ coatings at 1100 °C after heat treatment for different times (a) 15 h, (b) 25 h, (c) 45 h, (d) 70 h, (e) 100 h, and (f) 300 h.

4. Conclusion

The nanostructured zirconia coating consisted of two kinds of structures: the continuous molten phase and the loose microstructure. The average grain size of zirconia coating calculated from XRD increased with the rising of annealing temperature and time.

The very low activation energy is observed for the grain growth in the nanostructured zirconia coating within the annealing temperature range of 600–1150 °C. The lower activation energy may be attributed to the existence of micro-pores between the grains and the grain-rotation-induced grain coalescence mechanism. The present results are beneficial to the application of nanostructured TBC used in the gas-turbine and diesel engines at high temperatures.

Acknowledgement

This work is supported by the National Natural Science Foundation of China under the contact 50176005 and Program for New Century Excellent Talents in University (NCET).

References

[1] D.M. Zhu, R.A. Miller, Thermal conductivity and elastic modulus evolution of thermal barrier coatings under high heat flux conditions, J. Therm. Spray Technol. 9 (2000) 175.

[2] M. Gell, Application opportunities for nanostructured materials and coatings, Mater. Sci. Eng. A 204 (1995) 246.

[3] Y.Y. Zeng, S.W. Lee, L. Gao, C.X. Ding, Atmospheric plasma sprayed coatings of nanostructured zirconia, J. Eur. Ceram. Soc. 22 (3) (2002) 347–351.

[4] R.S. Lima, A. Kucuk, C.C. Berndt, Evaluation of microhardness and elastic modulus of thermally sprayed nanostructured zirconia coatings, Surf. Coat. Technol. 135 (2001) 166–172.

[5] H. Chen, C.X. Ding, Nanostructured zirconia coating prepared by atmospheric plasma spraying, Surf. Coat. Technol. 150 (1) (2002) 31–36.

[6] C.G. Zhou, N. Wang, S.K. Gong, H.B. Xu, Thermal cycling life and thermal diffusivity of a plasma-sprayed nanostructured thermal barrier coating, Scripta Mater. 51 (2004) 945–948.

[7] J. Karthikeyan, C.C. Berndt, J. Tikkanen, S. Reddy, H. Herman, Plasma spray synthesis of nanomaterial powders and deposits, Mater. Sci. Eng. A 238 (1997) 275–286.

[8] H.P. Klug, L.E. Alexander, X-ray Diffraction Procedures for Polystalline and Amorphous Materials, John Wiley & Sons, Inc., London, 1954,148–154.

[9] L.L. Shaw, D. Goberman, The dependency of microstructure and properties of nanostructured coatings on plasma spray conditions, Surf. Coat. Technol. 130 (2000) 1.

[10] T.G. Nigh, J. Wadsworth, Superplastic behaviour of a fine-grained yttria-stabilized tetragonal zirconia polycrystal(Y-TZP), Acta Metall. Mater. 38 (6) (1990) 1121–1133.

[11] S.G. Chen, Y.S. Yin, D.P. Wang, X. Wang, Effect of nanocrystallite structure on the lower activation energy for Sm_2O_3-doped ZrO_2, J. Mol. Struct. 703 (2004) 19–23.

[12] E.R. Leite, T.R. Giraldi, Crystal growth in colloidal tin oxide nanocrystals induced by coalescence at room temperature, Appl. Phys. Lett. 83 (8) (2003) 1566–1568.

[13] R.L. Penn, J.F. Banfield, Morphology development and crystal growth in nanocrystalline aggregates under hydrothermal conditions: insights from titania, Geochim. Cosmochim. Acta 63 (10) (1999) 1549–1557.